Inorganic Chemistry
Article

Inorg. Chem. **2009**, *48*, 8947–8954 **8947**
DOI: 10.1021/ic901196f

Synthesis, Structure, and Characterization of Two Photoluminescent Zirconium Phosphate−Quinoline Compounds

Lei Liu,[†] Jinping Li,[†] Jinxiang Dong,*[,†] Dubravka Šišak,[‡] Christian Baerlocher,[‡] and Lynne B. McCusker*[,‡]

[†]*Research Institute of Special Chemicals, Taiyuan University of Technology, Taiyuan, Shanxi 030024, People's Republic of China, and* [‡]*Laboratory of Crystallography, ETH Zurich, 8093 Zurich, Switzerland*

Received June 22, 2009

Two novel zirconium phosphate compounds, $|(C_9H_8N)_4(H_2O)_4|[Zr_8P_{12}O_{40}(OH)_8F_8]$ and $|(C_9H_8N)_2|[Zr_2P_2O_6(OH)_4F_4]$, designated as ZrPOF-Q1 and ZrPOF-Q2, respectively, have been synthesized hydrothermally in the presence of quinoline and HF and characterized by elemental and thermogravimetric analyses, UV−vis spectroscopy, and scanning electron microscopy. Their crystal structures were determined from powder X-ray diffraction data using a charge-flipping algorithm. The ZrPOF-Q1 structure [$P\bar{1}$, a=10.7567(1) Å, b=13.8502(1) Å, c=14.8995(1) Å, α=109.6(1)°, β=101.1(1)°, and γ=100.5(1)°] consists of zirconium phosphate layers with quinolinium ions in between. The layers are unusual in that isolated ZrO_2F_4 octahedra are anchored on both sides of the layer and protrude into the interlayer space. The ZrPOF-Q2 structure [$P\bar{1}$, a=7.7058(1) Å, b=12.3547(1) Å, c=6.5851(1) Å, α=97.0(1)°, β=89.7(1)°, and γ=101.9(1)°] consists of zirconium phosphate chains with an unusual Zr/P ratio of 1.0, interspersed with quinolinium ions. Both materials are stable up to 250 °C and exhibit interesting photoluminescence in the UV−vis spectral region. This is attributed to the protonated quinoline molecules, which are an integral part of both structures.

Introduction

Zirconium phosphates have been shown to have potential as proton conductors, ion exchangers, adsorbers, and catalysts,[1−3] so the preparation of new materials in this system with novel structures and/or chemical compositions is of considerable interest. Indeed, a series of zirconium phosphate materials with different dimensionalities, ranging from single or composite chains[4] to layer compounds[5] to open-framework structures,[6] have been prepared by introducing fluoride into the solvothermal synthesis procedure. In these syntheses, ammonium ions[4,7,8] and a variety of organic di- and triamines,[9−16] were used as structure-directing agents (SDAs).

Most studies of the zirconium phosphate system, however, have focused on the modification of the two well-known layer compounds, α-$Zr(HPO_4)_2\cdot H_2O$ (α-ZrP) and γ-$ZrPO_4(H_2PO_4)\cdot 2H_2O$ (γ-ZrP). A series of inorganic−organic functional derivatives have been produced using postprocessing techniques with these materials (e.g., ion exchange, intercalation, or infinite swelling).[17,18] By the selection of guest molecules with specific functions, zirconium phosphate materials with unique properties, such as fluorescence,[19] molecular or chiral recognition,[20] or catalysis,[21] have been designed.

*To whom correspondence should be addressed. E-mail: dongjinxiangwork@hotmail.com (J.D.), mccusker@mat.ethz.ch (L.B.M.). Telephone: +86-351-6010550-8 (J.D.), +41-44-632-3721 (L.B.M.). Fax: +86-351-6111178 (J.D.), +41-44-632-1133 (L.B.M.).

(1) Alberti, G.; Casciola, M.; Costantino, U.; Vivani, R. *Adv. Mater.* **1996**, *8*, 291.
(2) Clearfield, A.; Thakur, D. S. *Appl. Catal.* **1986**, *26*, 1.
(3) Brunet, E.; Alhendawi, H. M. H.; Cero, C.; de la Mata, M. J.; Juanes, O.; Rodríguez-Ubis, J. C. *Angew. Chem., Int. Ed.* **2006**, *45*, 6918.
(4) Gatta, G. D.; Masci, S.; Vivani, R. *J. Mater. Chem.* **2003**, *13*, 1215.
(5) Wloka, M.; Trojanov, S. I.; Kemnitz, E. *J. Solid State Chem.* **2000**, *149*, 21.
(6) Kemnitz, E.; Wloka, M.; Troyanov, S. I.; Stiewe, A. *Angew. Chem., Int. Ed. Engl.* **1996**, *35*, 2677.
(7) Wang, D.; Yu, R.; Takei, T.; Kumada, N.; Kinomura, N. *Chem. Lett.* **2002**, *31*, 398.
(8) Wang, D.; Yu, R.; Kumada, N.; Kinomura, N. *Chem. Lett.* **2002**, *31*, 804.
(9) Hursthouse, M. B.; Malik, K. M.; Thomas, J. M.; Chen, J.; Xu, J.; Song, T.; Xu, R. *Russ. Chem. Bull.* **1994**, *43*, 1787.
(10) Sung, H. H.-Y.; Yu, J.; Williams, I. D. *J. Solid State Chem.* **1998**, *140*, 46.
(11) Wang, D.; Yu, R.; Kumada, N.; Kinomura, N. *Chem. Mater.* **2000**, *12*, 956.
(12) Serre, C.; Taulelle, F.; Férey, G. *Solid State Sci.* **2001**, *3*, 623.
(13) Kumada, N.; Nakatani, T.; Yonesaki, Y.; Takei, T.; Kinomura, N. *J. Mater. Sci.* **2008**, *43*, 2206.
(14) Wloka, M.; Trojanov, S. I.; Kemnitz, E. *J. Solid State Chem.* **1998**, *135*, 293.
(15) Wloka, M.; Trojanov, S. I.; Kemnitz, E. *Solid State Sci.* **2002**, *4*, 1377.
(16) Wloka, M.; Trojanov, S. I.; Kemnitz, E. *Z. Anorg. Allg. Chem.* **1999**, *625*, 1028.
(17) Alberti, G.; Murcia-Mascarós, S.; Vivani, R. *J. Am. Chem. Soc.* **1998**, *120*, 9291.
(18) Nakayama, H.; Hayashi, A.; Eguchi, T.; Nakamura, N.; Tsuhako, M. *J. Mater. Chem.* **2002**, *10*, 3093.
(19) Bermúdez, R. A.; Colón, Y.; Tejada, G. A.; Colón, J. L. *Langmuir* **2005**, *21*, 890.
(20) Cao, G.; Garcia, M. E.; Alcalá, M.; Burges, L. F.; Mallouk, T. E. *J. Am. Chem. Soc.* **1992**, *114*, 7574.
(21) Santiago, M. B.; Declet-Flores, C.; Diaz, A.; Velez, M. M.; Bosques, M. Z.; Sanakis, Y.; Colon, J. L. *Langmuir* **2007**, *23*, 7810.

Published on Web 08/21/2009

Table 1. Synthesis Conditions Investigated

run	HF	$ZrOCl_2$	H_3PO_4	quinoline	H_2O	conditions	product
1	2	1	2	3	100	7 days, 180 °C	ZrPOF-Q1
2	3	1	2	3	100	7 days, 180 °C	ZrPOF-Q1 + α-ZrP
3	4	1	2	3	100	7 days, 180 °C	α-ZrP
4	4	1	1.5	4	100	7 days, 200 °C	ZrPOF-Q2
5	4	1	3	4	100	7 days, 200 °C	α-ZrP

We have now combined these two concepts by using a functional molecule as an SDA in a series of zirconium phosphate hydrothermal syntheses. This was a natural extension of our previous work in the $HF-ZrO_2-P_2O_5$–pyridine–H_2O system, which resulted in the open-framework zirconium phosphate $|(C_5H_6N)_4(H_2O)_2|[Zr_{12}P_{16}O_{60}(OH)_4F_8]$ (ZrPOF-pyr).[22] In that structure, protonated pyridine was found to be occluded in the channel. The $HF-ZrO_2-P_2O_5$–quinoline–H_2O system was considered to be attractive because quinoline (C_9H_7N) is closely related to pyridine and also exhibits fluorescence when photoexcited in the near-UV region. We hoped that this approach would not only produce new materials with useful properties but also provide a new strategy for the introduction of the desired functionality into a zirconium phosphate material. The study resulted in two new polycrystalline zirconium phosphate compounds with fluorescent properties. The two materials were then characterized by scanning electron microscopy, thermal gravimetric (TGA), and photoluminescence analyses, and their structures were determined from powder X-ray diffraction (PXRD) data.

Experimental Section

Raw Chemicals. Zirconium oxychloride ($ZrOCl_2 \cdot 8H_2O$, 99 wt %), *o*-phosphoric acid (H_3PO_4, 85 wt %), quinoline (C_9H_7N, 99 wt %), and hydrogen fluoride (HF, 40 wt %) were purchased from commercial sources and used in all syntheses without further purification.

Synthesis. The mineralizer HF is known to affect crystal growth and sometimes to act as an SDA.[6] Therefore, a series of syntheses in the $HF-ZrO_2-P_2O_5$–quinoline–H_2O system, in which particular attention was paid to the amount of HF added to the initial mixture, were performed (see Table 1). In this series, two novel materials, designated as ZrPOF-Q1 and ZrPOF-Q2, were produced. For ZrPOF-Q1, the molar ratio of the starting reactants was 2:1:1:3:100 $HF-ZrO_2-P_2O_5$–quinoline–H_2O, and for ZrPOF-Q2, it was 4:1:0.75:4:100 $HF-ZrO_2-P_2O_5$–quinoline–H_2O.

Typically, HF was added to an aqueous solution of $ZrOCl_2$ and the mixture stirred for about 10 min. With continuous stirring, phosphoric acid, followed by quinoline, was added to the solution. Once the mixture was homogeneous, it was poured into a 30 mL Teflon-lined stainless steel autoclave to approximately 70% of its capacity. The autoclave was then sealed and heated at either 180 or 200 °C for 7 days under autogenous pressure. The crystalline products were separated by centrifugation, washed with distilled water and then with ethanol, and dried at room temperature in air.

Characterization. The crystallinity, phase purity, and identity of the products were determined from PXRD patterns collected on a Rigaku D/max-2500 diffractometer. In situ high-temperature PXRD patterns were collected on a PANalytical XPERT PRO diffractometer under flowing air, using a HTK-16 attachment with a heating rate of 10 °C/min between scans. Both diffractometers were operated using Cu $K\alpha_1$ radiation ($\lambda = 1.5406$ Å).

The crystal morphology and size were checked with a JSM-6360LV scanning electron microscope. TGA curves were obtained on a Netzsch STA409C thermogravimetric analyzer in a nitrogen atmosphere with a heating rate of 10 °C/min over the temperature range 40–800 °C. The fluorescence spectra were measured at room temperature on a Hitachi F-4500 spectrofluorometer with a slit width for both the excitation and emission measurements of 5 nm. The powder sample was placed in a powder sample cell, which was then fitted into the metal-frame aperture. For the analysis, the optical axis was perpendicular to the powder surface (quartz window).

CHN analysis was carried out on an Elementar Vario EL analyzer, the fluoride content was determined using the fluoride-ion selective electrode method, and the zirconium and phosphorus contents were determined using a xylenol orange and phosphomolybdenum blue spectrophotometric method, respectively.

PXRD Data Collection. High-resolution synchrotron PXRD data were collected on both samples using the powder diffractometer on the Swiss–Norwegian Beamlines (SNBL) at the European Synchrotron Radiation Facility (ESRF) in Grenoble, France. High-resolution laboratory data were also collected on ZrPOF-Q2 using a Stoe STADI P diffractometer equipped with a linear (nominally 5 degrees) position-sensitive detector (PSD). Further details of the data collection parameters are given in Table 2.

Table 2. PXRD Data Collection Parameters for ZrPOF-Q1 and ZrPOF-Q2

	ZrPOF-Q1	ZrPOF-Q2	
instrument	SNBL at ESRF	Stoe STADI P	SNBL at ESRF
wavelength (Å)	0.500 07	Cu $K\alpha_1$	0.497 19
diffraction geometry	Debye–Scherrer	Debye–Scherrer	Debye–Scherrer
detector	Si(111) analyzer crystal	linear PSD	Si(111) analyzer crystal
sample	1.0 mm capillary	0.5 mm capillary	0.5 mm capillary
2θ range (deg)	2.0000–30.0000	5.00–99.99	2.100–40.000
step size 2θ (deg)	0.0025	0.01	0.002

Table 3. Chemical Analyses of ZrPOF-Q1 and ZrPOF-Q2

		C	H	N	Zr	P	F
ZrPOF-Q1	wt %	15.9	1.9	2.1	25.6	13.3	5.5
	molar	9.0	12.8	1.0	1.9	2.9	2.0
ZrPOF-Q2	wt %	28.6	2.6	3.7	23.7	7.9	9.5
	molar	9.0	9.8	1.0	1.0	1.0	1.9

Results

Chemical Analysis. The results of the chemical analyses are shown in Table 3. The molar ratios have been normalized to 9.0 C (i.e., one quinoline molecule).

Synthesis. As can be seen from Table 1, the amount of HF in the initial reaction mixture proved to be an important factor. Starting with the optimal synthesis conditions for ZrPOF-Q1 (run 1) but adding more HF to the initial mixture resulted in the formation of a significant amount of α-ZrP in addition to the ZrPOF-Q1 phase (run 2). At even higher HF concentrations, only α-ZrP was formed (run 3). Keeping this higher HF concentration but reducing the amount of H_3PO_4 and increasing the amount of quinoline (run 4) resulted in the formation of the second new zirconium phosphate phase ZrPOF-Q2. Starting with the previous mixture but increasing the amount of H_3PO_4 (run 5), however, led once again to the formation of α-ZrP. SEM micrographs of the two products are shown in Figure 1.

(22) Dong, J. X.; Liu, L.; Li, J.; Li, Y.; Baerlocher, Ch.; McCusker, L. B. *Microporous Mesoporous Mater.* **2007**, *104*, 185.

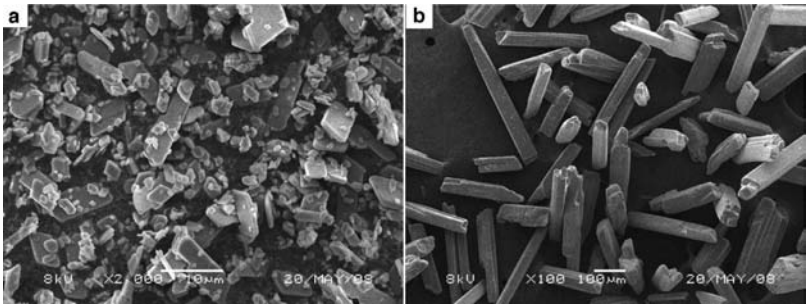

Figure 1. SEM micrographs of (a) ZrPOF-Q1 and (b) ZrPOF-Q2.

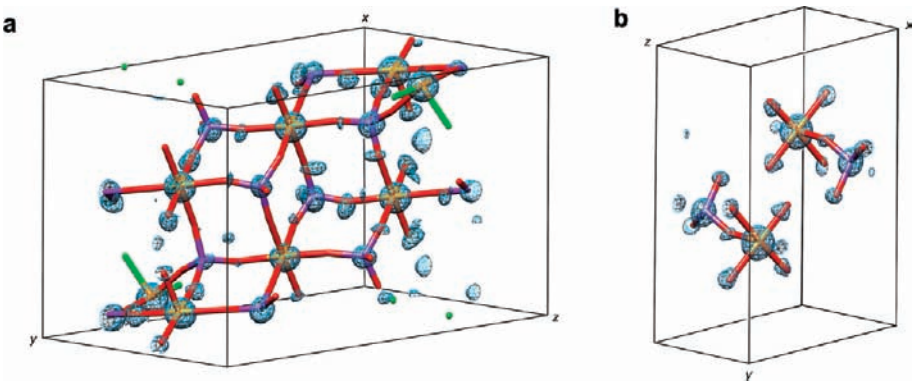

Figure 2. pCF electron density map for (a) ZrPOF-Q1 and (b) ZrPOF-Q2. A stick drawing of the final zirconium phosphate structure is overlaid for comparison (Zr, orange; P, purple; O, red; F, green).

Structure Solution. The PXRD patterns of both ZrPOF-Q1 and ZrPOF-Q2 were indexed with triclinic unit cells [ZrPOF-Q1, a = 10.7567(1) Å, b = 13.8502(1) Å, c = 14.8995(1) Å, α = 109.6(1)°, β = 101.1(1)°, γ = 100.5(1)°; ZrPOF-Q2, a = 7.7058(1) Å, b = 12.3547(1) Å, c = 6.5851(1) Å, α = 97.0(1)°, β = 89.7(1)°, γ = 101.9(1)°]. In both cases, reflection intensities were extracted from the PXRD pattern and then used as input to the powder charge-flipping (pCF) structure-solution algorithm that is implemented in the program *Superflip*.[23] The intensities for ZrPOF-Q1 were extracted from synchrotron data using the program *EXTRACT*[24] in the *XRS-82* suite of programs,[25] while those for ZrPOF-Q2 were extracted from laboratory data (synchrotron data had not yet been collected) using the program *GSAS*.[26] The structure of ZrPOF-Q2 is a much simpler than that of ZrPOF-Q1, so laboratory data were sufficient for the initial structure solution. However, higher quality synchrotron data were used for the final refinement of the structure. More information about the charge-flipping structure-solution algorithm can be found in ref 27 and that about the powder implementation in *Superflip* in ref 28. The input parameters for charge flipping that were used for ZrPOF-Q1 and ZrPOF-Q2 are given in Table 4.

Table 4. Charge-Flipping Input Parameters

	ZrPOF-Q1	ZrPOF-Q2
initial repartitioning with FIPS[29]	yes	no
chemical composition used for histogram matching (HM)	$Zr_6P_{12}O_{54}$	$Zr_2P_4O_{12}C_9NH_7$
first HM	after 21 cycles	after 21 cycles
subsequent HM	every 7 cycles	every 7 cycles
overlap factor (fwhm)	0.2	0.25
d_{min} (Å)	0.97	1.02
total reflections	4522	1218
overlapping reflections	3507	885
overlap groups	942	255
runs	100	100
cycles per run	205	205

ZrPOF-Q1. The 20 best electron density maps produced by *Superflip* were shifted to the same origin and examined by eye. Eight of these with similar features were averaged (Figure 2a), and the highest peaks in this map could be interpreted as a zirconium phosphate layer similar to that in α-ZrP (layer of ZrO_6 octahedra linked to one another via corner-sharing PO_4 tetrahedra to form a layer with terminal P−OH groups on both sides). Additional isolated ZrO_6 octahedra appeared to be anchored via P−O bonds on both sides of the layer.

ZrPOF-Q2. The 10 best electron density maps produced by *Superflip* all looked very similar (Figure 2b), showing chains of octahedra and tetrahedra that could be interpreted easily as corner-sharing ZrO_6 and PO_4 species. No clearly defined electron density from quinoline molecules was apparent.

(23) Palatinus, L.; Chapuis, G. *J. Appl. Crystallogr.* **2007**, *40*, 786.
(24) Baerlocher, Ch. *EXTRACT: A Fortran program for the extraction of integrated intensities from a powder pattern*; Institut für Kristallographie, ETH: Zürich, Switzerland, 1990.
(25) Baerlocher, Ch.; Hepp, A. *XRS-82. The X-ray Rietveld System*; Institut für Kristallographie, ETH: Zürich, Switzerland, 1982.
(26) Larson, A. C.; Von Dreele, R. B. *General Structure Analysis System* (*GSAS*); Los Alamos National Laboratory Report LAUR 86-748; Los Alamos National Laboratory: Los Alamos, NM, 2000.
(27) Oszlányi, G.; Sütő, A. *Acta Crystallogr., Sect. A* **2008**, *64*, 123.
(28) Baerlocher, Ch.; McCusker, L. B.; Palatinus, L. *Z. Kristallogr.* **2007**, *222*, 47.
(29) Estermann, M. A.; Gramlich, V. *J. Appl. Crystallogr.* **1993**, *26*, 396.

Structure Refinement. In both cases, the zirconium phosphate unit derived from the charge-flipping solution was used to start Rietveld refinement using the *XRS-82* suite of programs.[24] The geometries of the partial structures were optimized, and then the missing atoms were located via a series of difference electron density maps.

ZrPOF-Q1. In the case of ZrPOF-Q1, it was not clear whether or not the pCF solution was centrosymmetric, so Rietveld refinement was initiated assuming the space group $P1$ and using a model consisting of 8 Zr, 12 P, and 46 O atoms. Successive difference maps then revealed the positions of two quinoline and two water molecules in the interlayer space. Geometric restraints were placed on the atoms of the zirconium phosphate layer, and subsequent refinement indicated that the structure was indeed centrosymmetric, so the space group was changed to $P\bar{1}$ and the number of parameters could be halved. Approximate geometric restraints were placed on the atoms of the organic molecules (all C at this point) and their positions refined. The N atoms were then identified as those making the closest approaches to an O atom of the zirconium phosphate layer, and then the geometric restraints were adjusted accordingly. For charge balance, the quinoline molecule had to be protonated, so the restraints were derived from several quinolinium salt structures in the Cambridge Structural Database.[30] The positions of the H atoms were calculated at the end of the refinement using the program *Mercury*[31] and added to the structural model to account for the (minor) scattering from these atoms but were not refined. It is generally very difficult to distinguish F^- and OH^- with X-rays because they both have 10 electrons, so chemical reasoning must be used. Chemical analysis showed that there are eight F atoms per unit cell. Of the 24 O atoms in the zirconium phosphate layer, the 4 terminal O atoms (8 per unit cell) on the zirconium octahedra protruding into the interlayer space appeared to be the most likely locations for these F atoms, so they were changed from O to F. Refinement of this 60-atom model (4 Zr, 6 P, 24 O, 4 F, 2 O_w, 18 C, and 2 N atoms) converged with the R values, $R_F = 0.054$ and $R_{wp} = 0.145$ ($R_{exp} = 0.154$).

ZrPOF-Q2. For ZrPOF-Q2, the initial refinement was performed using laboratory data. Because the pCF solution appeared to be centrosymmetric, Rietveld refinement was started assuming the space group $P\bar{1}$ and using a model consisting of one Zr, one P, and seven O atoms. The positions of the atoms of a quinoline molecule were then located between the zirconium phosphate chains. At this point, synchrotron data had been collected, so the refinement was continued with these. As for ZrPOF-Q1, the N atom of the quinolidium ion was identified, the geometric restraints were adjusted accordingly, and the positions of the H atoms were calculated. Chemical analysis of this material showed that there are four F atoms per unit cell, but it was not clear where these were most likely to be located because there are six terminal Zr−O atoms per unit cell. In view of the fact that it is virtually impossible to distinguish F and OH with X-rays, all were left as O atoms. Refinement of this 19-atom model (one Zr, one P, seven O, nine C, and one N atoms) converged with the R values, $R_F = 0.056$ and $R_{wp} = 0.149$ ($R_{exp} = 0.152$).

For both stuctures, all atoms were refined isotropically, and the displacement parameters for similar atoms were constrained to be equal to keep the number of parameters

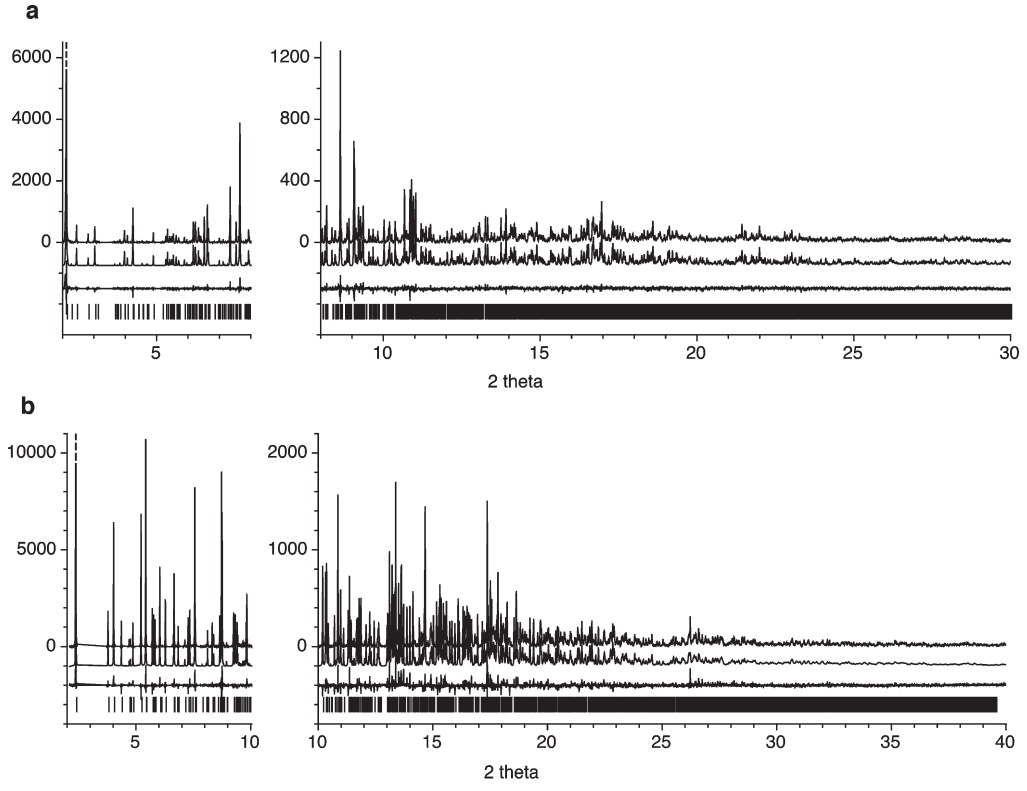

Figure 3. Observed (top), calculated (middle), and difference (bottom) profiles for the Rietveld refinement of (a) ZrPOF-Q1 and (b) ZrPOF-Q2. In both cases, the first peak has been cut at approximately half-height and the profiles for the higher angles have been scaled up by a factor of 5 to show more detail. Tick marks indicate the positions of the reflections.

Table 5. Crystallographic Data for ZrPOF-Q1 and ZrPOF-Q2

	ZrPOF-Q1	ZrPOF-Q2
chemical composition	$\|(C_9H_8N)_4(H_2O)_4\|$ $[Zr_8P_{12}O_{40}(OH)_8F_8]$	$\|(C_9H_8N)_2\|$ $[Zr_2P_2O_6(OH)_4F_4]$
unit cell		
a (Å)	10.7567(1)	7.7060(1)
b (Å)	13.8502(1)	12.3550(1)
c (Å)	14.8995(1)	6.5850(1)
α (deg)	109.6(1)	97.0(1)
β (deg)	101.1(1)	89.7(1)
γ (deg)	100.5(1)	101.9(1)
space group	$P\bar{1}$	$P\bar{1}$
d_{min} (Å)	0.97	0.73
contributing reflns	4606	3200
geometric restraints	218	61
Zr−O/F	24	6
P−O	24	4
O/F−ZrO/F	60	15
O−P−O	36	6
Zr−O−P	20	3
C−C/C−N	22	11
C−C−C/ C−N−C/ C−C−N	32	16
structural param	186	62
profile param	10	10
R_F	0.054	0.056
R_{wp}	0.145	0.149
R_{exp}	0.154	0.152

to a minimum. Neutral scattering factors were used for all atoms. Details of the refinements are given in Table 5. The final atomic parameters for the two structures are provided as CIF files (see the Supporting Information). Fits of the profiles calculated from the final models to the experimental data are shown in Figure 3.

TGA. The TGA curves for ZrPOF-Q1 and ZrPOF-Q2 are shown in Figure 4. The former consists of three main steps with weight losses of ~2.5% between room temperature and 200 °C, ~6.7% between 200 and 300 °C, and ~12.9% between 300 and 450 °C. Above 450 °C, there is a further, gradual weight loss of ~3.1% (Figure 4). The TGA curve for ZrPOF-Q2 also exhibits three main steps, but these are between 200 and 350 °C, between 350 and 450 °C, and between 450 and 600 °C, with weight losses of ~24.7%, ~6.9%, and ~9.0%, respectively. Above 600 °C, there is a gradual weight loss of ~1.7%. In situ high-temperature PXRD measurements show that both structures are stable up to 250 °C and undergo phase transitions at higher temperatures (Figure 5).

Fluorescence. Figure 6 shows the photoluminescence spectra of ZrPOF-Q1 and ZrPOF-Q2 obtained with an excitation wavelength of 250 nm. A well-structured fluorescence band with a maximum at ca. 388 nm is observed for both zirconium phosphate materials. The spectra are similar to that observed for quinolinium in a quinolinium chloride solution.[32,33]

Discussion

Structure. ZrPOF-Q1. The structure of ZrPOF-Q1 can be described in terms of zirconium phosphate layers in the xy plane, centered at $z = {}^1/_2$, separated by layers of quinolinium ions and water molecules (Figure 7). The

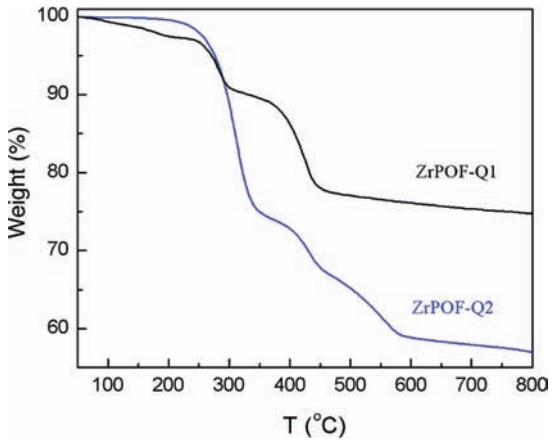

Figure 4. TGA curves for ZrPOF-Q1 and ZrPOF-Q2.

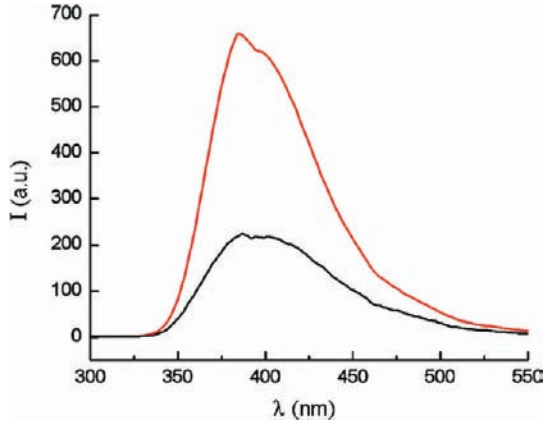

Figure 6. Photoluminescence spectra for ZrPOF-Q1 (black) and ZrPOF-Q2 (red) ($\lambda_{ex} = 250$ nm).

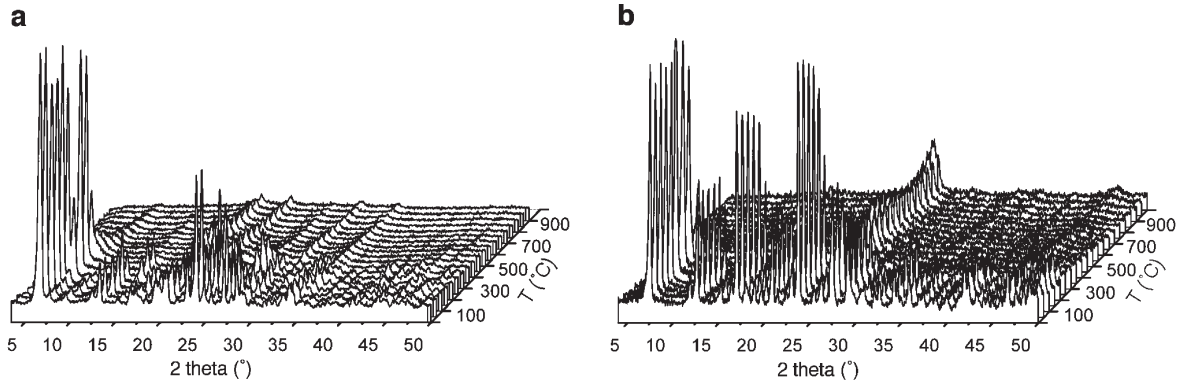

Figure 5. PXRD patterns of (a) ZrPOF-Q1 and (b) ZrPOF-Q2 collected in situ as a function of the temperature.

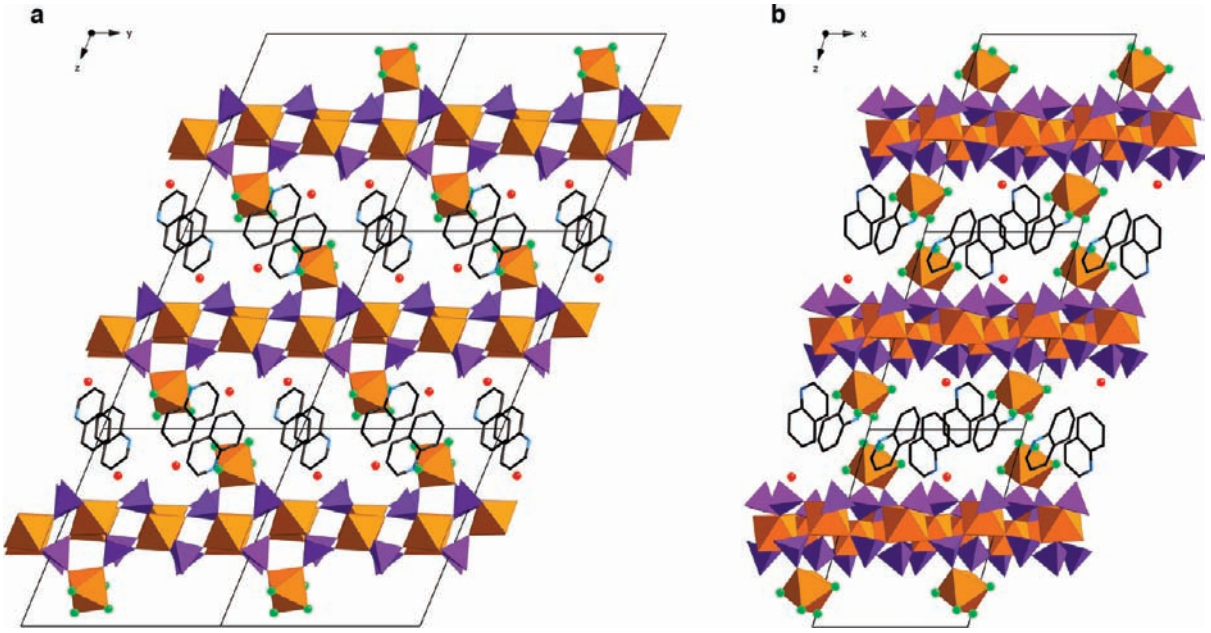

Figure 7. Projections of the structure of ZrPOF-Q1 (a) along the [100] direction and (b) along the [010] direction (PO_4, purple; $Zr(O/F)_6$, orange; F, green; C, black; N, blue; water, red). Note the short F···F distances between adjacent layers.

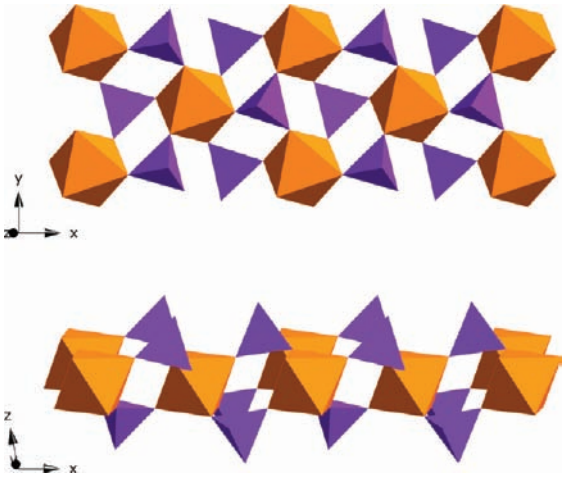

Figure 8. Top and side views of the zirconium phosphate layer in α-$Zr(HPO_4)_2 \cdot H_2O$ (α-ZrP) (PO_4, purple; ZrO_6, orange).

inorganic layer is similar to that found in α-ZrP (Figure 8), with ZrO_6 octahedra linked to one another on both sides via corner-sharing, 3-connected PO_4 tetrahedra. However, in ZrPOF-Q1, additional, isolated ZrO_2F_4 octahedra are also anchored to the phosphate outer layers via oxygen bridges. These octahedra protrude into the interlayer space, and indeed the closest distance between the terminal F atoms in adjacent layers is only 3.1 Å, making it a *pseudo*-three-dimensional framework.

The protonated quinoline molecules are arranged in pairs at the unit cell corners (quin1) and at the center of the *ab* plane (quin2) (Figure 9). The two molecules of the pairs are related by centers of symmetry and are aligned parallel to one another at a distance of ca. 3.6 Å. The different orientations of the quin1 and quin2 pairs can be seen in Figure 9. Each of the four terminal P−OH groups of the zirconium phosphate layer is a hydrogen-bonding distance from either a water molecule (O···O = 2.62 and 2.64 Å), the N atom of a quin2 quinolinium ion (N···O = 2.87 Å), or one of the terminal Zr−F atoms (O···F = 2.54 Å). The quin1 quinolinium ion is 2.57 Å from a different terminal F atom.

ZrPOF-Q2. The structure of ZrPOF-Q2 consists of rows of simple ladderlike zirconium phosphate chains separated by layers of quinolinium ions (Figure 10). The chains have an unusual Zr/P ratio of 1.0, with each ZrO_4F_2 octahedron connected to three P atoms via O bridges and each PO_4 tetrahedron, in turn, connected to three Zr atoms. The chains run parallel to the *c* axis and are arranged in rows along the *a* axis. Neighboring chains are connected to one another via strong hydrogen bonds between the terminal P−OH groups and a terminal Zr(O/F) atom (O···O/F = 2.50 Å). The quinolinium ions lie in between these layers and, as in ZrPOF-Q1, are arranged in pairs separated by ca. 3.6 Å. The N atom of each quinolinium ion approaches a terminal Zr(O/F) atom at 2.68 Å.

Chemical Composition. The chemical analyses shown in Table 3 are consistent with the two structures. For ZrPOF-Q1, the molar ratios calculated from the structure are 9:12:1:2:3:2 C/H/N/Zr/P/F (measured: 9:12.8:1.0:1.9:2.9:2.0), and those for ZrPOF-Q2 are 9:10:1:1:1:2 C/H/N/Zr/P/F (measured: 9:9.8:1.0:1.0:1.0:1.9). It is interesting to note that, although ZrPOF-Q1 was synthesized from a reaction mixture with a F/Zr/P/quinoline ratio of 2:1:2:3, the final structure has the ratio 2:2:3:1. In the case of ZrPOF-Q2, the reaction mixture had a ratio of 4:1:1.5:4 and the final structure 2:1:1:1.

Synthesis. The crystal structure of ZrPOF-Q1 has an F/Zr ratio of 1.0 (2.0 used in the synthesis mixture), whereas

(30) Allen, F. H. *Acta Crystallogr., Sect. B* **2002**, *58*, 380.
(31) Macrae, C. F.; Bruno, I. J.; Chisholm, J. A.; Edgington, P. R.; McCabe, P.; Pidcock, E.; Rodriguez-Monge, L.; Taylor, R.; van de Streek, J.; Wood, P. A. *J. Appl. Crystallogr.* **2008**, *41*, 466.
(32) Anton, M. F.; Moomaw, W. R. *J. Chem. Phys.* **1977**, *66*, 1808.
(33) Moomaw, W. R.; Anton, M. F. *J. Phys. Chem.* **1976**, *80*, 2243.

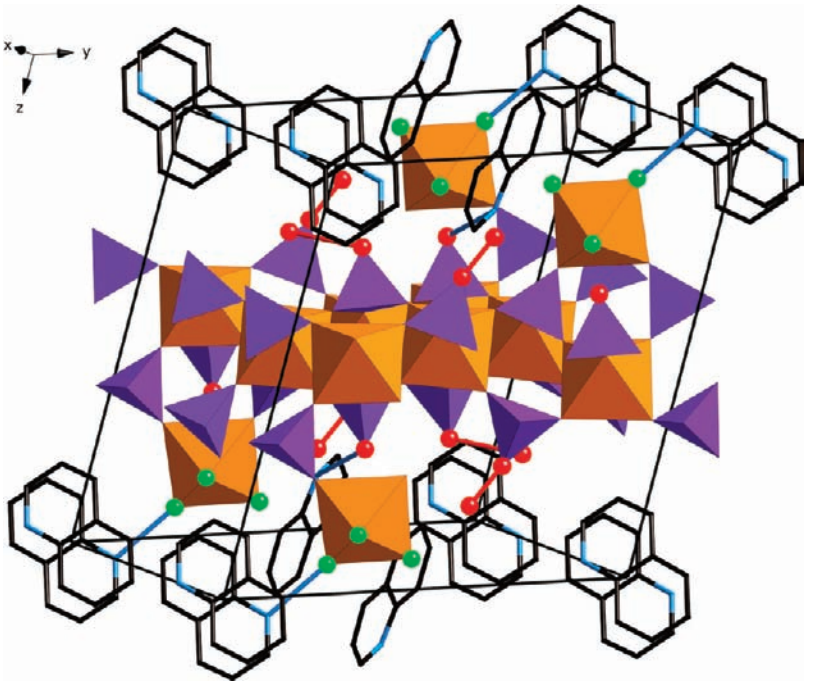

Figure 9. Structure of ZrPOF-Q1 showing the interactions between the O and F atoms of the zirconium phosphate layer with the interlayer quinolinium ions and water molecules (PO_4, purple; $Zr(O/F)_6$. orange; F, green; C, black; N, blue; O, red). Note the different orientations of the quin1 (at the corners of the unit cell) and the quin2 (at the center of the *ab* plane) pairs of quinolinium ions.

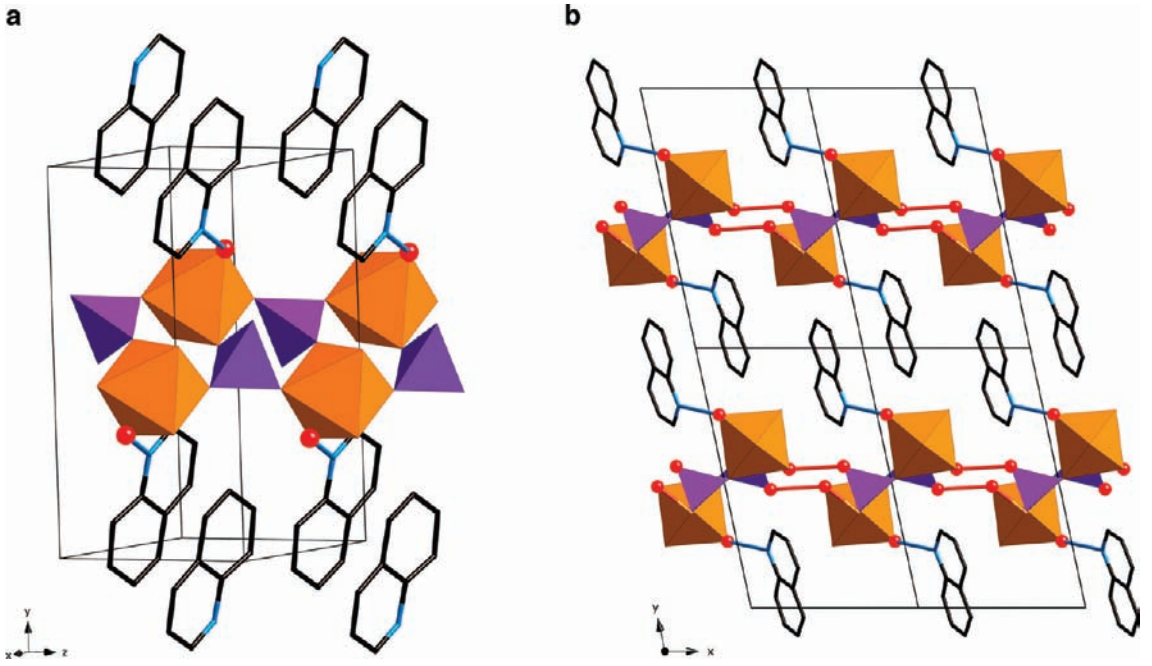

Figure 10. Structure of ZrPOF-Q2 showing (a) the zirconium phosphate chain and its interaction with the quinolinium ions and (b) the hydrogen bonding (red lines) between the chains along the *x* axis (PO_4, purple; $Zr(O/F)_6$, orange; C, black; N, blue; O, red).

that of ZrPOF-Q2 has an F/Zr ratio of 2.0 (4.0 in the synthesis mixture). It seems that a higher F/Zr ratio promotes lower-dimensional zirconium phosphate units in the final structure. The morphologies of the two compounds (see Figure 1) are consistent with their framework dimensionalities. The two-dimensional zirconium phosphate ZrPOF-Q1 grows as thin plates, with the longest dimension being several micrometers, while the one-dimensional ZrPOF-Q2 grows as rodlike crystals, with the longest dimension being over 100 μm.

TGA. The first 2.5% weight loss in the TGA curve for ZrPOF-Q1 is attributed to the loss of the four water molecules per unit cell (calcd 2.7%), and the second and third steps (19.6% weight loss) are assigned to the loss/decomposition of the four quinoline molecules (calcd 19.8%). The final weight loss above 450 °C probably corresponds to the loss of HF from the structure, which gives rise to the concomitant phase transformation.

As might be expected, the ZrPOF-Q2 phase does not show any appreciable weight loss below 200 °C because

there is no water in the structure. The first two steps (31.6% weight loss) account for almost all of the quinoline species in the structure (calcd 35.0%), and the loss above 450 °C corresponds approximately to the residual quinoline and HF.

The PXRD patterns in Figure 5 show quite clearly that both structures are stable up to 250 °C. This is in stark contrast to the quinolinium salts. The melting point of quinolinium chloride, for example, is just 134 °C. This means that the fluorescent properties of these two compounds could be exploited in a much broader temperature range than could those of a simple quinolinium salt.

Fluorescence. The photoluminescence observed in these two zirconium phosphates can be attributed to the protonated quinoline species, which balance the charge of the zirconium phosphate layers in ZrPOF-Q1 and chains in ZrPOF-Q2. The difference in emission intensity at λ_{max} = 388 nm for the two materials reflects the different amounts of quinolinium in the structures (20 wt % for ZrPOF-Q1 vs 35 wt % for ZrPOF-Q2). Further measurements to probe the temperature dependence of the photoluminescence are planned. It should be noted that the fluorescence λ_{max} for these two compounds has a blue shift with respect to that for quinolinium ions in an aqueous solution (ca. 400 nm). This is consistent with the more rigid environment of the quinolinium ions in these solid materials (rigidochromic effect).[34,35] It is also observed for methylviologen (MV^{2+})-exchanged α-ZrP, which has a λ_{max} of 337 nm versu 350 nm for MV^{2+} in an acetonitrile solution.[36] By contrast, the photoluminescence spectrum of the layered zirconium phosphate $|Co(dien)_2(H_2O)_3|[Zr_4H_8P_5O_{26}]$ (ZrPO-CJ37), excited at 243 nm, shows wide and distinct emission bands at 300, 380−430, and 450−600 nm. These are attributed to a charge transfer from oxygen to zirconium in the octahedral $Zr(OM)_6$ (M = P, H) moiety in the inorganic layer.[37] To the best our knowledge, this is the first report of a hydrothermal synthesis of a zirconium phosphate with photoluminescence.

Conclusions

Two novel zirconium phosphate fluorides, ZrPOF-Q1 ($|C_9H_8N)_4(H_2O)_4|[Zr_8P_{12}O_{40}(OH)_8F_8]$) and ZrPOF-Q2 ($|(C_9H_8N)_2|[Zr_2P_2O_6(OH)_4F_4]$), have been synthesized hydrothermally in the presence of HF and quinoline. Quinoline was selected as the SDA in the hope that its photoluminescent properties would also be found in the final product. ZrPOF-Q1 has a unique layer structure with isolated ZrO_2F_4 octahedra anchored via P−O−Zr linkages on both sides of an α-ZrP-type layer. These octahedra, with four terminal F atoms, protrude into the interlayer space, and those of adjacent layers approach one another at 3.1 Å to form a *pseudo*-three-dimensional framework structure. ZrPOF-Q2 has an unusual chain structure with a P/Zr ratio of 1. This ratio has not been observed in any other one-dimensional zirconium phosphate compounds. The chains are hydrogen-bonded to one another to form a layer, and the quinolinium ions fill the interlayer space. As hoped, both materials exhibit photoluminescence in the UV−vis spectral region, and this is attributed to the presence of protonated quinoline in the two crystal structures. The stronger emission from ZrPOF-Q2 is consistent with its higher quinolinium content (35 wt % vs 20 wt % for ZrPOF-Q1). This new strategy for the synthesis of zirconium phosphate materials, using a functional organic compound as an SDA in a hydrothermal synthesis, offers new perspectives for the synthesis of materials with specific functionality and novel structures.

Acknowledgment. We thank the beamline scientists at the SNBL at the ESRF in Grenoble, France, for their assistance with the PXRD measurements. The Chinese group was financially supported by the National Natural Science Foundation (Grants 20825623 and 20801039) and the Shanxi Natural Science Foundation for Young Scientists (Grant 2008021014). The Swiss group was funded, in part, by the Swiss National Science Foundation.

Supporting Information Available: Crystallographic information files in CIF format for ZrPOF-Q1 and ZrPOF-Q2. This material is available free of charge via the Internet at http://pubs.acs.org.

(34) Trobajo, C.; Khainakov, S. A.; Espina, A.; García, J. R. *Chem. Mater*. **2000**, *12*, 1787.
(35) Wrighton, M.; Morse, D. L. *J. Am. Chem. Soc*. **1974**, *96*, 998.
(36) Martí, A. A.; Paralitici, G.; Maldonado, L.; Colón, J. L. *Inorg. Chim. Acta* **2007**, *360*, 1535.
(37) Du, Y.; Pan, Q.; Li, J.; Yu, J.; Xu, R. *Inorg. Chem*. **2007**, *46*, 5847.